ECLÉTICA QUÍMICA

Eclet. Quim. 51 | e-1570, 2026

Original Article, Education in Chemistry and Correlated Areas

https://doi.org/10.26850/1678-4618.eq.v51.2026.e1570

Synthesis of chitosan/AC/Fe_3O_4 nanocomposite and its structural, magnetic, and heavy metal adsorption characteristics

Berliana Ayu **Febrianti**[1], Herlin **Pujiarti**[1], Ulfawanti Intan **Subadra**[1], Ahmad **Taufiq**[1+]

Abstract

The chitosan/activated carbon (AC)/Fe_3O_4 nanocomposite has been successfully synthesized. The nanocomposite was then characterized to investigate its structural, magnetic, and heavy metal Cr(III) adsorption characteristics using XRD, SEM, FTIR, VSM, and ICP-OES. The chitosan/AC/Fe_3O_4 nanocomposite performed a single phase with a cubic inverse spinel structure with a lattice parameter and crystallite size of 8.38 ± 0.01 Å and 5.04 ± 0.09 nm, respectively. The SEM image showed that the morphology of chitosan/AC/Fe_3O_4 tended to be spherical with an average particle size of 51.4 ± 0.4 nm. The FTIR spectrum showed that the chitosan/AC/Fe_3O_4 nanocomposite exhibited the presence of a β-1,4-glycosidic bond at 858 cm^{-1} originating from chitosan. The C=C functional group and Fe-O bonds appeared at 1606 and 439–642 cm^{-1}, indicating the presence of AC and Fe_3O_4. The chitosan/AC/Fe_3O_4 nanocomposite had superparamagnetic properties with a saturation magnetization value of 36.27 ± 0.05 emu/g. Furthermore, the chitosan/AC/Fe_3O_4 nanocomposite had a capacity and efficiency for Cr(III) adsorption of 13.95 mg/g and 27.88% at a contact time of 240 min, respectively.

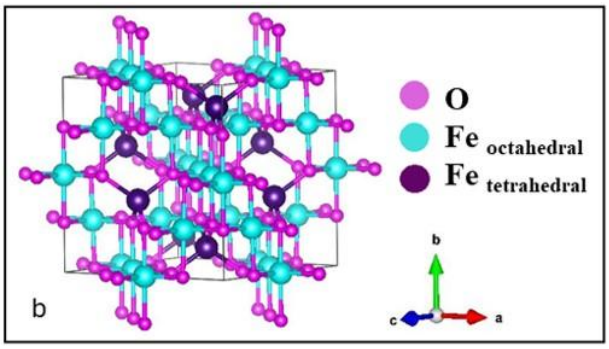

Article History

Received	May 19, 2024
Accepted	March 07, 2025
Published	March 04, 2026

Keywords

1. nanocomposite;
2. chitosan/AC/Fe_3O_4;
3. cubic inverse spinel;
4. saturation magnetization;
5. heavy metal Cr(III) adsorption.

Section Editors

Manuel Ignacio Azocar **Guzmán**

Highlights

- Chitosan/AC/Fe_3O_4 was synthesized using coprecipitation and sol-gel methods.
- Chitosan/AC/Fe_3O_4 demonstrated capacity and efficiency to adsorb heavy metals.
- Adsorption of chromium(III) at 240 min contact was 13.95 mg/g and 27.88%.

[1]State University of Malang, Faculty of Mathematics and Natural Science, Malang, Indonesia. **+Corresponding author:** Ahmad Taufiq, **Phone:** +6281233196644, **Email address:** ahmad.taufiq.fmipa@um.ac.id

1. Introduction

In recent years, chromium waste pollution caused by industrial development has become a concern because of its significant impact on human health (Amjad *et al.*, 2020), such as skin irritation, kidney problems, digestive disorders, and lung cancer (Khanduri, 2020; Xiong *et al.*, 2023). Therefore, to address these problems, developing wastewater treatment strategies is crucial. In the last few decades, nanoparticle-based adsorption methods have been widely developed due to their flexibility, economy, and effectiveness (Lakherwal, 2014). In this regard, due to their large surface area, chitosan nanoparticles are one of the materials that are widely used to overcome heavy metal ion pollution, namely chitosan nanoparticles, so that they provide very good adsorption (Zhang *et al.*, 2021). This is important because the adsorption performance is highly dependent on the particle surface area, which has been empirically demonstrated in previous research, where the adsorption capacity increased from 368 to 1500 mg/g along with the increase in surface area from 858 to 3022 m^2/g (Xu *et al.*, 2015). In this context, chitosan has advantages related to the amino and hydroxyl groups contained in it, making it effective as an adsorption site (Wang, K. *et al.*, 2023). However, despite these advantages, chitosan still has low mechanical strength and selectivity, and is easily soluble in acids, which limits its performance (Larasati *et al.*, 2022). Based on this explanation, it is important to propose a solution through the incorporation of other materials such as activated carbon (AC) to improve its characteristics.

Engineering through the incorporation of AC is important because it has the advantages of pores and a large surface area (Gao *et al.*, 2020), thus showing good adsorbent performance (Nejadshafiee and Islami, 2019). Furthermore, AC also has other advantages for use as an adsorptive material because it has various important functional groups (Heidarinejad *et al.*, 2020). However, for the benefit of advanced applications that require superior adsorption performance, further engineering with other materials is also important through a combination of Fe_3O_4 nanoparticles. This is important because these nanoparticles have a large surface area to improve their performance (Liu *et al.*, 2020), including the advantage of strong magnetic properties. In this research, the synthesis of AC and Fe_3O_4 is proposed using natural resources from coconut shells and iron sand.

2. Experimental

2.1. Synthesis

In this research, materials such as HCl, H_2O, NH4OH, HNO_3, iron sand, shrimp, and coconut shells were used in the synthesis process. Specifically, Fe_3O_4 was synthesized using iron sand by reacting with HCl to obtain a solution, followed by reaction with NH_4OH (Febrianti *et al.*, 2023). To obtain Fe_3O_4 nanoparticle powder, the resulting product was then washed repeatedly and heated at a temperature of 100 °C. Meanwhile, charcoal obtained from coconut shells was prepared through a combustion process at a temperature of 400 °C in the AC synthesis process (Saputra *et al.*, 2021). Next, HNO_3 was used to react with the combustion product, followed by a repeated washing process. In more detail, the process of making chitosan/AC/Fe_3O_4 nanocomposite followed previous research (Utami *et al.*, 2023).

2.2. Characterization

The characterization was carried out using X-ray diffraction (XRD) to determine crystallite sizecrystal structure. Scanning electron microscopy (SEM) was employed to determine the sample's morphology and particle size. Fourier-transform infrared (FTIR) spectroscopy was employed to determine the functional groups. A vibrating sample magnetometer (VSM) was applied to determine the sample's magnetic properties. Then, inductively coupled plasma-optical emission spectrometry (ICP-OES) was used to determine the adsorption performance for heavy metal chromium.

3. Results and Discussion

Figure 1a shows the x-ray diffraction pattern of the chitosan/AC/Fe_3O_4 nanocomposite with diffraction peaks appearing at 2θ = 30.11°, 35.48°, 43.13°, 53.49°, 57.12°, and 62.73°, which represent hkl planes (220), (311), (400), (422), (511), and (440), respectively. Based on the results of data analysis, it is known that the resulting diffraction peaks were related to the diffraction pattern of magnetite (Fe_3O_4). Structurally, this material forms a cubic spinel system. Examining Fig. 1b, it can be seen that the Fe^{3+} ions in Fe_3O_4 occupy tetrahedral and octahedral sites. Interestingly, the Fe^{2+} ions only occupy octahedral sites which are structurally an inverse spinel type. The results of data analysis also show that the diffraction peaks of AC and chitosan are not detected, which conceptually means that both do not form a cubic crystalline system but are amorphous (Bai *et al.*, 2018; Hu *et al.*, 2018; Juang *et al.*, 2018). In general, the results of this study show a similar pattern to the results of previous studies, especially related to the diffraction peak pattern of AC, Fe_3O_4, and chitosan (Çavuşoğlu *et al.*, 2019). The particle size of Fe_3O_4 was 5.04 ± 0.09 nm with the lattice parameter of 8.38 ± 0.01 Å.

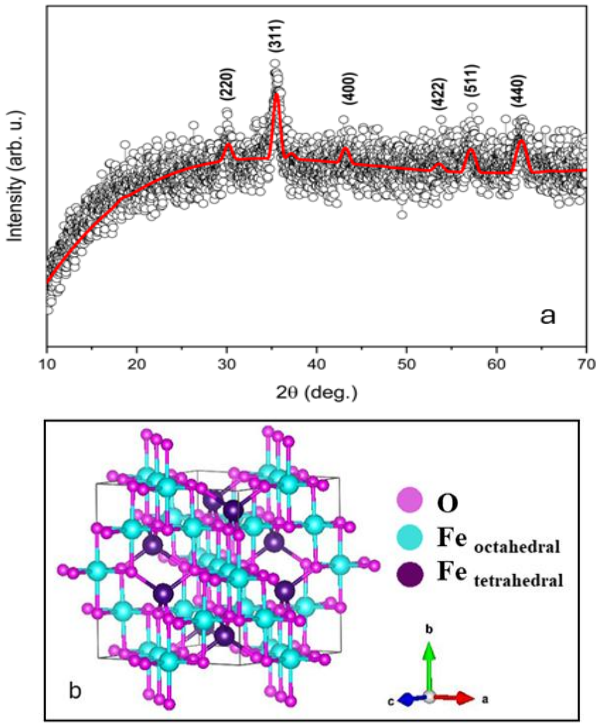

Figure 1. (a) X-ray diffraction pattern and **(b)** crystal structure of chitosan/AC/Fe_3O_4 nanocomposite.
Source: Elaborated by the authors.

The morphology of the chitosan/AC/Fe_3O_4 nanocomposite is shown in **Fig. 2a**. Nanocomposites consist of spherical particles and tend to agglomerate. Agglomeration is caused by magnetic forces so that the particles attract each other (Modaresi *et al.*, 2019; Wang, H. and Shadman, 2013). The particle size distribution of the nanocomposite was 51 nm (**Fig. 2b**). The particle size is still in the nano category, so it has a high affinity and is advantageous for adsorbing heavy metals (Peng *et al.*, 2016).

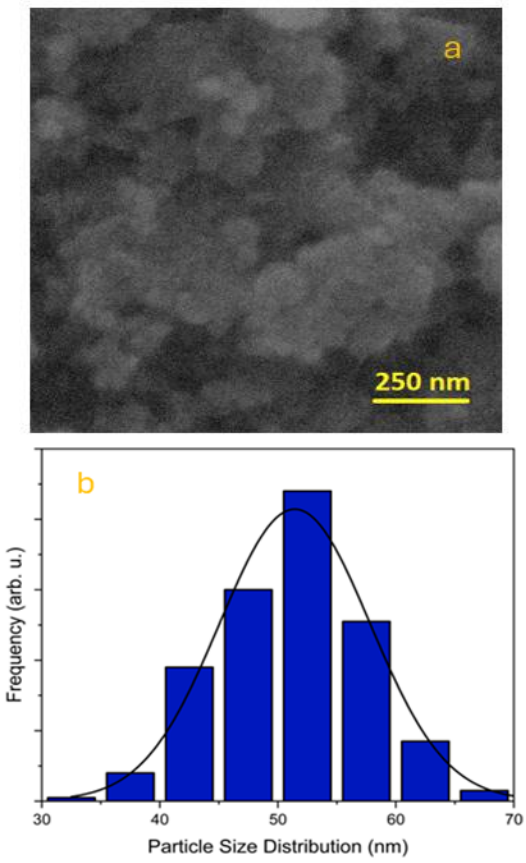

Figure 2. (a) Morphology and **(b)** particle size distribution of chitosan/AC/Fe_3O_4 nanocomposite.
Source: Elaborated by the authors.

The FTIR spectrum of the chitosan/AC/Fe_3O_4 nanocomposite is shown in **Fig. 3** with a wavenumber range from 4000 to 400 cm^{-1}. Based on the results, it can be shown that the stretching and bending of the O–H functional groups were detected at 3304 cm^{-1} (Peng *et al.*, 2016). Then, the alkane group appeared around 2308 cm^{-1}, indicating the presence of stretching vibrations on the C-H functional groups (Munasir and Kusumawati, 2019). Moreover, the C=C functional group was detected at 1606 cm^{-1}, as the main functional group of carbon (Muraleedharan *et al.*, 2015). In general, the analysis results show that the main functional groups of AC, chitosan, and Fe_3O_4 were detected as evidence of the successful synthesis of chitosan/AC/Fe_3O_4 nanocomposite. In more detail, this can be seen from the C–O functional group detected at 1257 and 1062 cm^{-1} (Munasir and Kusumawati, 2019). Meanwhile, the H–O–H functional group was detected at 392 and 1606 cm^{-1}). The stretching vibration of the β–1,4–glycosidic bond appeared at 858 cm^{-1}, as a characteristic bond of chitosan. Furthermore, the Fe–O functional group was detected at 439 cm^{-1} and 640 cm^{-1} (Malega *et al.*, 2018), which showed vibrations in the octahedral and tetrahedral positions, respectively.

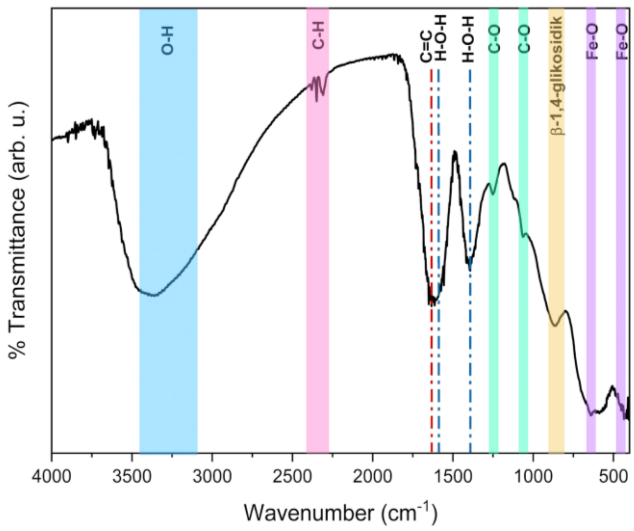

Figure 3. Spectrum of chitosan/AC/Fe_3O_4 nanocomposite.
Source: Elaborated by the authors.

In addition to the characterization of the crystal structure and functional groups, magnetic characterization was also carried out in this study, the results of which are in the form of an M–H hysteresis curve in **Fig. 4**. The hysteresis curve was analyzed quantitatively and produced a saturation magnetization (Ms) of 36.27 ± 0.05 emu/g. The results of this analysis, when compared with previous studies (Liu *et al.*, 2016), showed a much smaller value. The decrease in the saturation magnetization value is predicted due to the addition of diamagnetic materials from AC and chitosan (Gholami *et al.*, 2019; Komlev *et al.*, 2018). Other quantitative analyses also show that the nanocomposite synthesized in this study has a coercivity field and remanent magnetization of 0.02 T and 0.01 emu/g, respectively, indicating superparamagnetic characteristics (Rampengan and Tompunu Tengker, 2021). Therefore, the chitosan/AC/Fe_3O_4 nanocomposite has a high potential for application in various fields.

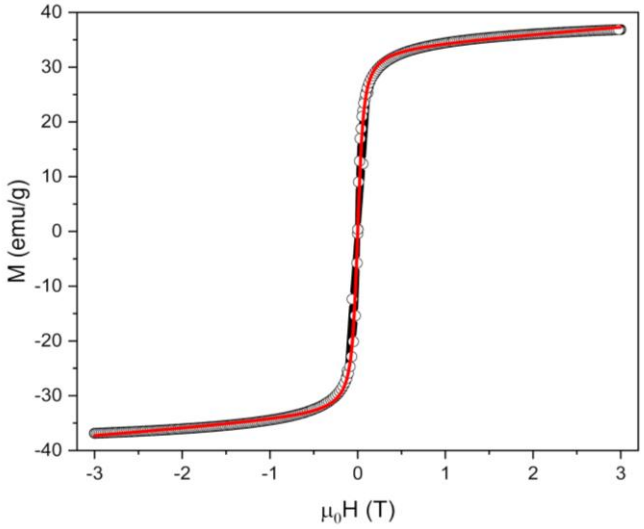

Figure 4. M–H hysteresis curve of chitosan/AC/Fe_3O_4 nanocomposite.
Source: Elaborated by the authors.

The heavy metal adsorption characterization of chitosan/AC/Fe_3O_4 nanocomposite was carried out at various contact times of 60, 120, 180, and 240 min, where the results are shown in **Fig. 5**. Based on the characterization results, the maximum values of adsorption capacity and efficiency were achieved at 13.95 mg/g and 27.88%, respectively, at a contact time of 240 min, as shown in **Table 1**. Interestingly, when compared with the results of previous research (Ahmad *et al.*, 2015), the performance of the nanocomposite from this research (13.95 mg/g) showed a better value than the adsorption capacity of pure chitosan, which was only 11.6 mg/g. Furthermore, the research conducted by Bernard *et al.* (2013) also showed that AC had an adsorption capacity and efficiency of 3.22 mg/g and 26.15%, respectively. Xue *et al.* (2021) also showed an adsorption capacity of Fe_3O_4 of 11.30 mg/g. The chitosan/AC/Fe_3O_4 nanocomposite exhibited a higher capacity and efficiency as an adsorbent than those of previous studies. Therefore, chitosan/AC/Fe_3O_4 nanocomposites synthesized from natural materials also have great potential for application as adsorption of heavy metals, especially chromium.

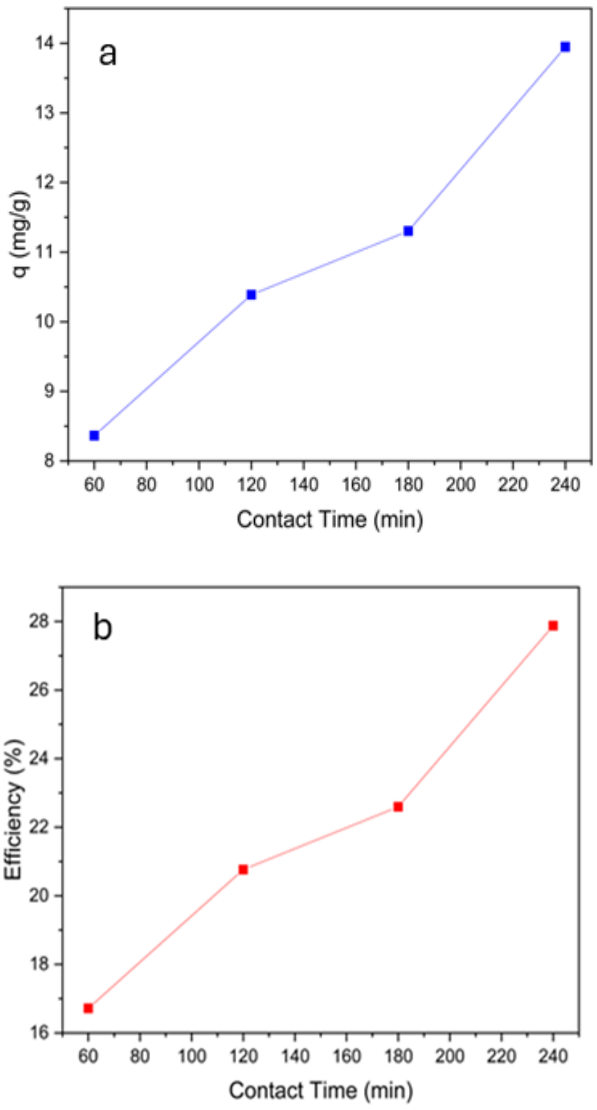

Figure 5. Graph of contact time relationship to **(a)** capacity and **(b)** adsorption efficiency of chromium metal by chitosan/AC/Fe_3O_4 nanocomposite.
Source: Elaborated by the authors.

Table 1. Table of contact time relationship to capacity and adsorption efficiency of chromium metal by chitosan/AC/Fe_3O_4 nanocomposite.

t (m)	Cr_0 (ppm)	Cr_t (ppm)	q (mg/g)	Efficiency (%)
60	100.06	83.33	8.36	16.72
120	100.06	79.29	10.39	20.76
180	100.06	77.46	11.30	22.59
240	100.06	72.17	13.95	27.88

Source: Elaborated by the authors.

4. Conclusions

The chitosan/AC/Fe_3O_4 nanocomposite for the adsorption of heavy metals has been successfully synthesized. The XRD characterization confirmed that the chitosan/AC/Fe_3O_4 nanocomposite had a single crystalline phase, namely Fe_3O_4, with an inverse cubic spinel structure with a crystal size of 5.04 ± 0.09 nm. The nanocomposite was composed of imperfectly spherical particles with a size of 51.4 ± 0.4 nm. The presence of chitosan and AC materials was confirmed by the vibrations of the β–1,4–glycosidic and C=C bonds at wavenumber 858 and 1606 cm^{-1}, respectively. The chitosan/AC/Fe_3O_4 nanocomposite had superparamagnetic properties with a saturation magnetization value of 36.27 ± 0.05 emu/g. Furthermore, for the adsorption of heavy metals, the chitosan/AC/Fe_3O_4 nanocomposite had a capacity and efficiency of 13.95 mg/g and 27.88%, respectively, at a contact time of 240 min.

Authors' contribution

Conceptualization: Ahmad Taufiq; **Data curation:** Berliana Ayu Febrianti; Ulfawanti Intan Subadra; **Formal Analysis:** Ahmad Taufiq; Herlin Pujiarti; **Funding acquisition:** Ahmad Taufiq; **Investigation:** Berliana Ayu Febrianti; Ulfawanti Intan Subadra; **Methodology:** Berliana Ayu Febrianti; Ulfawanti Intan Subadra; **Project administration:** Ulfawanti Intan Subadra; **Resources:** Berliana Ayu Febrianti; Ulfawanti Intan Subadra; **Software:** Ulfawanti Intan Subadra; Herlin Pujiarti; **Supervision:** Herlin Pujiarti; Ahmad Taufiq; **Validation:** Ulfawanti Intan Subadra; Ahmad Taufiq; **Visualization:** Berliana Ayu Febrianti; Ulfawanti Intan Subadra; **Writing – original draft:** Herlin Pujiarti; Ahmad Taufiq; **Writing – review & editing:** Berliana Ayu Febrianti; Ulfawanti Intan Subadra; Ahmad Taufiq.

Conflict of interest

The authors declare that there is no conflict of interest.

Data availability statement

The data will be available upon request.

Artificial Intelligence usage statement

The authors declare that no AI tools were used in the scientific development of this manuscript; only minor spelling checks were performed using standard language editing software.

Funding

This work was supported by a Research Scheme "Publikasi Skripsi" from Universitas Negeri Malang for AT with grant number 5.4.410/UN32.20.1/LT/2023.

Acknowledgments

The authors acknowledge the Physics Laboratory and the Central Laboratory staff of Universitas Negeri Malang for technical assistance in synthesis and characterization.

References

Ahmad, M.; Ahmed, S.; Ikram, S. Adsorption of Heavy Metal Ions: Role of Chitosan and Celulose for Water Treatment. *Int. J. Pharmacogn.* **2015**, *2* (6), 280–289. https://doi.org/10.13040/IJPSR.0975-8232.IJP.2(6).280-89

Amjad, M.; Hussain, S.; Javed, K.; Khan, A. R.; Shahjahan, M. The Sources, Toxicity, Determination of Heavy Metals and Their Removal Techniques from Drinking Water. *World J. Appl. Chem.* **2020**, *5* (2), 34–40. https://doi.org/10.11648/j.wjac.20200502.14

Bai, B.; Xu, X.; Li, C.; Xing, J.; Wang, H.; Suo, Y. Magnetic Fe_3O_4@Chitosan carbon microbeads: Removal of doxycycline from aqueous solutions through a fixed bed via sequential adsorption and heterogeneous fenton-like regeneration. *J. Nanomater.* **2018**, *2018*, 5296410, https://doi.org/10.1155/2018/5296410

Bernard, E.; Jimoh, A.; Obofoni Odigure, J. Heavy metals removal from industrial wastewater by activated carbon prepared from coconut shell. *Res. J. Chem. Sci.* **2013**, *3* (8), 3–9.

Çavuşoğlu, F. C.; Akan, S.; Arı, E. A.; Çetinkaya, E.; Çolak, E.; Daştan, G. N.; Deniz, S.; Erdem, D.; Köksal, M.; Korkmaz, S.; Onsekiz, N.; Oruçoğlu, B.; Özkaya, D.; Uslu, H. B.; Ünal, Ç.; Yıldız, O.; Özkara-Aydınoğlu, Ş.; Bayazit, Ş. S. Preparation of magnetic activated carbon-chitosan nanocomposite for crystal violet adsorption. *Korean J. Chem. Eng.* **2019**, *36* (11), 1915–1921. https://doi.org/10.1007/s11814-019-0377-9

Febrianti, N. S.; Taufiq, A.; Hidayat, A.; Mufti, N.; Subadra, S. U. I. Synthesis and Characterization of $ZnFe_2O_4$-PEG/RGO Nanocomposites as Lead Heavy Metal Adsorbents. *Key Eng. Mater.* **2023**, *941*, 155–163. https://doi.org/10.4028/p-d8u8p7

Gao, Y.; Yue, Q.; Gao, B.; Li, A. Insight into activated carbon from different kinds of chemical activating agents: A review. *Sci. Total Environ.* **2020**, *746*, 141094. https://doi.org/10.1016/j.scitotenv.2020.141094

Gholami, M.; Zare-Hoseinabadi, A.; Mohammadi, M.; Taghizadeh, S.; Behzad Behbahani, A.; Amani, A. M.; Solghar, R. A. Preparation of $Zn_xFe_{3-x}O_4$@chitosan Nanoparticles as an Adsorbent for Methyl Orange and Phenol. *J. Environ. Treat. Tech.* **2019**, *7* (3), 245–249.

Heidarinejad, Z.; Dehghani, M. H.; Heidari, M.; Javedan, G.; Ali, I.; Sillanpää, M. Methods for preparation and activation of activated carbon: a review. *Environ. Chem. Lett.* **2020**, *18* (2), 393–415. Springer. https://doi.org/10.1007/s10311-019-00955-0

Hu, H.; Yang, L.; Lin, Z.; Xiang, X.; Jiang, X.; Hou, L. Preparation and characterization of novel magnetic Fe_3O_4/chitosan/$Al(OH)_3$ beads and its adsorption for fluoride. *Int. J. Biol. Macromol.* **2018**, *114*, 256–262. https://doi.org/10.1016/j.ijbiomac.2018.03.094

Juang, R. S.; Yei, Y. C.; Liao, C. S.; Lin, K. S.; Lu, H. C.; Wang, S. F.; Sun, A. C. Synthesis of magnetic Fe_3O_4/activated carbon nanocomposites with high surface area as recoverable adsorbents. *J. Taiwan Inst. Chem. Eng.* **2018**, *90*, 51–60. https://doi.org/10.1016/j.jtice.2017.12.005

Khanduri, P. Environmental Hazards and Crisis Management for Sustainable Development. *Int. J. Sci. Res.* **2020**, *10* (11), 1386–1389. https://doi.org/10.21275/SR211126123651

Komlev, A.; Lähderanta, E.; Shevchenko, E.; Vorob'ev-Desyatovskii, N. Magnetism of purified amorphous carbon. *EPJ Web Conf.* **2018**, *185*, 04012. https://doi.org/10.1051/epjconf/201818504012

Lakherwal, D. Adsorption of Heavy Metals: A Review. *Int. J. Environ. Res. Dev.* **2014**, *4* (1), 41–48.

Larasati, I.; Wijayanti, D.; Widhi Mahatmanti, F.; Kimia, J.; Matematika, F.; Ilmu, D.; Alam, P. Synthesis of Chitosan/Activated Carbon Composite Beads as an Adsorbent of Pb(II) and Cu(II) ions in Aqueous Solution: A Review. *Indones. J. Chem. Sci.* **2022**, *11* (2), 190–197. https://doi.org/10.15294/ijcs.v11i2.54943

Liu, G.; Li, T.; Yang, X.; She, Y.; Wang, M.; Wang, J.; Zhang, M.; Wang, S.; Jin, F.; Jin, M.; Shao, H.; Jiang, Z.; Yu, H. Competitive fluorescence assay for specific recognition of atrazine by magnetic molecularly imprinted polymer based on Fe_3O_4-chitosan. *Carbohydr. Polym.* **2016**, *137*, 75–81. https://doi.org/10.1016/j.carbpol.2015.10.062

Liu, S.; Yu, B.; Wang, S.; Shen, Y.; Cong, H. Preparation, surface functionalisation and application of Fe_3O_4 magnetic nanoparticles. *Adv. Colloid Interface Sci.* **2020**, *281*, 102165. https://doi.org/10.1016/j.cis.2020.102165

Malega, F.; Indrayana, I. P. T.; Suharyadi, E. Synthesis and Characterization of the Microstructure and Functional Group Bond of Fe_3O_4 Nanoparticles from Natural Iron Sand in Tobelo North Halmahera. *J. Ilm. Pendidik. Fis. Al-Biruni.* **2018**, *7* (2), 129–138. https://doi.org/10.24042/jipfalbiruni.v7i2.2913

Modaresi, N.; Afzalzadeh, R.; Aslibeiki, B.; Kameli, P.; Ghotbi Varzaneh, A.; Orue, I.; Chernenko, V. A. Magnetic properties of $Zn_xFe_{3-x}O_4$ nanoparticles: A competition between the effects of size and Zn doping level. *J. Magn. Magn. Mater.* **2019**, *482*, 206–218. https://doi.org/10.1016/j.jmmm.2019.03.060

Munasir.; Kusumawati, R. P. Synthesis and Characterization of Fe_3O_4@rGO Composite with Wet-Mixing (ex-situ) Process. *J. Phys.: Conf. Ser.* **2019**, *1171* (1), 012048. https://doi.org/10.1088/1742-6596/1171/1/012048

Muraleedharan, K.; Alikutty, P.; Abdul Mujeeb, V. M.; Sarada, K. Kinetic Studies on the Thermal Dehydration and Degradation of Chitosan and Citralidene Chitosan. *J. Polym. Environ.* **2015**, *23*, 1–10. https://doi.org/10.1007/s10924-014-0665-8

Nejadshafiee, V.; Islami, M. R. Adsorption capacity of heavy metal ions using sultone-modified magnetic activated carbon as a bio-adsorbent. *Mater. Sci. Eng. C.* **2019**, *101*, 42–52. https://doi.org/10.1016/j.msec.2019.03.081

Peng, B.; Song, T.; Wang, T.; Chai, L.; Yang, W.; Li, X.; Li, C.; Wang, H. Facile synthesis of Fe_3O_4@$Cu(OH)_2$ composites and their arsenic adsorption application. *Chem. Eng. J.* **2016**, *299*, 15–22. https://doi.org/10.1016/j.cej.2016.03.135

Rampengan, A. M.; Tompunu Tengker, S. M. Analisa Sifat Kemagnetan Polimer Poliethylen Glycol (PEG-4000)-coated Nanopartikel Magnetite Fe_3O_4 Menggunakan Vibrating Sample Magnetometer (VSM). *Fullerene J. Chem.* **2021**, *6* (2), 161–164. https://doi.org/10.37033/fjc.v6i2.376

Saputra, K.; Sunaryono, S.; Hidayat, S.; Wisodo, H.; Taufiq, A. Investigation of nanostructural and magnetic properties of $Mn_{0.25}Fe_{2.75}O_4$/AC nanoparticles. *Mater. Today Proc.* **2021**, *44*, 3350–3354. https://doi.org/10.1016/j.matpr.2020.11.646

Utami, R.; Taufiq, A.; Sunaryono, S.; Nikmah. Preliminary studies on magnetite/HA/chitosan nanocomposite: Nanostructure and drug loading characteristics. *AIP Conf. Proc.* **2023**, *2634* (1), 020035. https://doi.org/10.1063/5.0112185

Wang, H.; Shadman, F. Effect of particle size on the adsorption and desorption properties of oxide nanoparticles. *AIChE J.* **2013**, *59* (5), 1502–1510. https://doi.org/10.1002/aic.13936

Wang, K.; Zhang, F.; Xu, K.; Che, Y.; Qi, M.; Song, C. Modified magnetic chitosan materials for heavy metal adsorption: a review. *RSC Adv.* **2023**, *13*, 6713–6736. https://doi.org/10.1039/d2ra07112f

Xiong, H.; Xu, J.; Li, S.; Xu, Y. Chromium(III) adsorption removal from acidic solutions by isomeric and tunnel-structural iron oxyhydroxides. *Water Sci. Technol.* **2023**, *87* (5), 1140–1158. https://doi.org/10.2166/wst.2023.049

Xu, F.; Tang, Z.; Huang, S.; Chen, L.; Liang, Y.; Mai, W.; Zhong, H.; Fu, R.; Wu, D. Facile synthesis of ultrahigh-surface-area hollow carbon

nanospheres for enhanced adsorption and energy storage. *Nat. Commun.* **2015**, *6*, 7221. https://doi.org/10.1038/ncomms8221

Xue, S.; Xiao, Y.; Wang, G.; Fan, J.; Wan, K.; He, Q.; Gao, M.; Miao, Z. Adsorption of heavy metals in water by modifying Fe_3O_4 nanoparticles with oxidized humic acid. *Colloids Surf. A Physicochem. Eng. Asp.* **2021**, *616*, 126333. https://doi.org/10.1016/j.colsurfa.2021.126333

Zhang, Y.; Zhao, M.; Cheng, Q.; Wang, C.; Li, H.; Han, X.; Fan, Z.; Su, G.; Pan, D.; Li, Z. Research progress of adsorption and removal of heavy metals by chitosan and its derivatives: A review. *Chemosphere*. **2021**, *279*, 130927. https://doi.org/10.1016/j.chemosphere.2021.130927